

Review

# Modeling Strategies for Crude Oil-Induced Fouling in Heat Exchangers: A Review

Obaid ur Rehman <sup>1,2</sup>, Marappa Gounder Ramasamy <sup>3</sup>, Nor Erniza Mohammad Rozali <sup>1,\*</sup>, Shuhaimi Mahadzir <sup>1</sup>, Ali Shaan Manzoor Ghumman <sup>1</sup> and Abdul Hannan Qureshi <sup>1</sup> 

<sup>1</sup> Department of Chemical Engineering, Universiti Teknologi PETRONAS, Seri Iskandar 32610, Perak, Malaysia

<sup>2</sup> Department of Chemical Engineering, University of Karachi, Karachi 75270, Pakistan

<sup>3</sup> Department of Chemical Engineering, KPR Institute of Engineering and Technology, Arasur, Coimbatore 641407, India

\* Correspondence: erniza.rozali@utp.edu.my; Tel.: +60-53-687-582

**Abstract:** Semi-empirical fouling models have proven more effective in predicting the fouling behavior of crude oils in heat exchangers. These models have aided refineries in optimizing operating conditions to minimize or eliminate fouling in preheat exchangers. Despite their complexity, the models continue to improve in approximating real behavior by taking into account previously neglected aspects. This paper summarizes these findings from various studies along with highlighting different factors which were considered to enhance the predictability of the models. A critical analysis is presented to emphasize that activation energy in the deposition term varies depending on the physical processes involved and may not conform to the precise definition of activation energy. Two primary modeling approaches for crude oil fouling have emerged, i.e., deterministic and threshold models. Threshold models have gained more attention due to their fewer adjustable parameters. The stability or compatibility of crude oils has a substantial impact on asphaltene deposition, which is a major contributor to fouling. However, incorporating this factor into fouling models has received little attention. The inclusion of parameters for inorganic fraction and ageing has increased predictability by accurately estimating the fouling thickness. The use of CFD to analyze fouling mechanisms is promising, particularly for complex geometries. The dynamic and moving boundary modeling approach has potential to broaden the applicability of fouling models.

**Keywords:** fouling; crude oil; heat exchanger; modeling; thermal-hydraulic; CFD



**Citation:** Rehman, O.u.; Ramasamy, M.G.; Rozali, N.E.M.; Mahadzir, S.; Ghumman, A.S.M.; Qureshi, A.H. Modeling Strategies for Crude Oil-Induced Fouling in Heat Exchangers: A Review. *Processes* **2023**, *11*, 1036. <https://doi.org/10.3390/pr11041036>

Academic Editors: Kiran Siddappaji, Erik Bartuli and Tereza Kudelova

Received: 10 February 2023

Revised: 17 March 2023

Accepted: 22 March 2023

Published: 29 March 2023



**Copyright:** © 2023 by the authors. Licensee MDPI, Basel, Switzerland. This article is an open access article distributed under the terms and conditions of the Creative Commons Attribution (CC BY) license (<https://creativecommons.org/licenses/by/4.0/>).

## 1. Introduction

The energy conservation in refinery is mainly attributed to the efficiency of preheat trains which are employed to extract the heat from side products and pumparounds to preheat the crude stream [1]. Reducing energy consumption by recovering the waste heat is promising for protection of the environment [2]. The buildup of the crude oil fouling layer, which manifests as insulation, on the walls of heat exchangers in refinery preheat trains resist the energy transfer that reduces the temperature downstream. The loss of energy is compensated by the fired heater and, in extreme cases, loss of production [3,4]. To overcome this problem, cleaning schedules have been commonly employed in refineries which appends the labor, cleaning chemicals, and waste disposal expenses to fouling cost [5]. The severity of the fouling problem can also be comprehended in terms of greenhouse gas emissions, which is related to the extra energy consumption for maintaining the coil outlet temperature [6,7].

The fouling process in preheat trains is governed by the deposition of organic material and inorganic constituents, especially sulfur and iron paralleled with a chemical reaction (autoxidation and condensation reactions) and insoluble particle deposition [8]. Generally, a significant proportion of foulants include asphaltenes deposits with small quantities of

corrosion products and inorganic material [9]. The factors affecting the fouling process are depicted in the Graphical Abstract.

For the past two decades, mathematical modeling of the fouling mechanism has been a major interest of researchers. The complexity in modeling arises from the variation in crude oil composition, resulting in the domination of one of the fouling mechanisms over another and the ageing of the deposit [10]. Another type of complexity is related to applying the model results to the field data because of the use of different operating parameters, and the geometry of the test equipment used [11].

The most widely used fouling prediction approach is to express the fouling rate using empirical or semi-empirical models [8]. Threshold fouling has been the most popular concept that describes the quantitative evaluation of the initial fouling rate [12]. It defines fouling mechanism in a robust manner by the inclusion of both deposition and removal phenomena. The recent research trend mainly focused on incorporating other mechanisms such as deposit ageing [13], hydraulic effects [14], asphaltene deposition [15,16], inorganic deposition [17], mass transfer [18,19], and the compatibility effect of crude oils [20–22].

Although excellent reviews are available in the literature on the understanding and evolution of crude oil fouling models [10,12,23–27], this work mainly focuses on examining newly developed modeling approaches in terms of robustness and predictability. In addition, the discussion has encompassed the impact of ageing and inorganic components, the thermal-hydraulic relationship, as well as the results of CFD investigations.

## 2. Deterministic Fouling Models

The deterministic models for fouling prediction were developed by many researchers based on a physical analysis of the fouling process. The term deterministic was used by Wilson et al. [12] to differentiate between models other than threshold fouling models; however, all these semi-empirical models were developed by physical evaluation of the fouling process. Kern and Seaton [28] were the first to propose the theory of fouling rate. They described the net fouling rate as the difference between deposition and removal rates. They also developed a prediction model for the thickness of the foulant layer. The model equation is:

$$dm/dt = \dot{m}_D - \dot{m}_R \quad (1)$$

$$dx/dt = k_m c J - k_r \tau x \quad (2)$$

The model was later improved by Watkinson [29], who introduced the sticking probability ( $B$ ) in the deposition term. He identified a weakness in Kern and Seaton's model, i.e., at higher velocities, no deposition would be achieved as the removal term depends on the deposit thickness. Epstein [30] developed a model in which chemical reaction fouling was considered a function of foulant residence time on the surface. The model later showed excellent agreement with the experimental data of Crittenden et al. [31] for heavy crude oil fouling in a circulation loop apparatus. However, it did not apply to crude oil fouling, due to the complex nature of crude oil and the difficult identification of fouling precursors. Paterson and Fryer [32] proposed a model for fouling by milk denaturation in which they consider the laminar sub-layer as a chemical reactor. The fouling rate was taken as the product of foulant production and sticking probability. The model involves many empirical quantities that are difficult to determine for crude oil application.

Later, Chambon et al. [33] reported good accuracy of the model for industrial heat exchanger fouling data. However, the correlation of deposition term with crude oil composition and heat exchanger geometry was missing. Joshi [34] proposed an empirical model in which the fouling ageing was introduced along with the asymptotic surface roughness parameter. The model showed good fitting of the data produced from a pilot plant heat exchanger; however, it introduced so many parameters that it would be difficult to find a good approximation. Rammerstorfer et al. [18] developed a model based on reaction kinetics. They ignored the suppression term in the fouling rate equation by considering only the

low shear stress conditions. They assumed that there is only one rate-limiting step among diffusion, adsorption, corrosion, chemical reaction, and asphaltene precipitation. They found that the first or second-order adsorption model was the rate-limiting step ruling out the possibility of other steps. The model showed a good approximation with experimental results of Watkinson [35], Scarborough et al. [36], Polly et al. [37], and Yang et al. [38] at surface temperatures from 573–673 K. The asphaltene precipitation step was excluded from consideration because model fouling rate decreased with increasing surface temperature, which contradicts experimental results. The effect of bulk temperature on asphaltene precipitation was not considered in this study. A chronological list of deterministic models is presented in Table 1.

**Table 1.** List of deterministic fouling models in chronological order.

Model	Author (s), Year & Ref.	Fluid	Operating Parameters	Equipment	Notes
$\frac{dm}{dt} = \dot{m}_D - \dot{m}_R$ $\frac{dx}{dt} = k_m c_f - k_r \tau x$	Kern & Seaton, 1959 [28]	Water	N/A	Heat exchanger	Introduced the basic concept of fouling Share based removal term
$\frac{dx}{dt} = k_m JB - k_r \tau x$	Watkinson, 1968 [29]	Sour heavy gas oil	$T_b = 366$ K $T_s = 477$ K $u = 1.7\text{--}7.4$ m/s	Heated tube	Introduced sticking probability
$r_f = \alpha \exp(-E/RT)/u$	Patterson, 1988 [32]	Skimmed milk	$T_b = 333$ K $T_s = 358\text{--}383$ K	Heated tube	Assumed sub-layer as a differential chemical reactor
$\frac{dR_f}{dt} = \alpha \exp(-E/RT_w)$	Crittenden et al., 1992 [39]	Crude oil	$T_b = 403$ K $T_s = 433\text{--}553$ K $u = 0.7\text{--}2.1$ m/s	Heat exchanger	
$\phi = \frac{\left. \frac{dR_f}{dt} \right _{t=0} = \frac{\alpha \phi}{\lambda_f \rho_f}}{\left( \frac{\beta S_c^{2/3}}{u_c \tau_f^{1/2}} \right) + \left( \frac{\gamma \rho u^2 c_f}{\mu \exp(-E/RT_{s0}) c_s^{n-1}} \right)}$	Epstein, 1994 [30]	Crude oil	N/A	Heated tube	Introduced residence time of foulant on the surface.
$R_f = \alpha \tau^{-\beta} S(t) / \lambda_f \rho_c$ $\lambda_f = (\lambda_\infty - \alpha \exp(-\gamma t T_s)) (\lambda_\infty - \lambda_c)$	Joshi, 2013 [34]	Crude oil	$u = 0.9\text{--}2.7$ m/s	Heat exchanger	Included both surface roughness and ageing parameters.
$\frac{dR_f}{dt} = \frac{M_f}{\lambda_f \rho_f} \cdot \exp(-E/RT_f) \cdot (c_{t,0} - c_{A,s}) \cdot c_{As}$	Rammerstorfer, 2019 [18]	Crude oil	N/A	N/A	Determined that fouling is adsorption controlled

The table also provides information on the experimental setup such as operating parameters, type of equipment and fluid used for the fouling study. Key notes are also added in the last column.

### 3. Threshold Fouling Models

The concept of the threshold fouling model was first introduced by Ebert and Panchal [40], which provides a semi-empirical approach to model linear initial fouling rate. They showed model validity based on the experimental data for tube side coking by Scarborough et al. [36]. In contrast to the deterministic models, which predict the asymptotic fouling resistance, the threshold fouling model aimed to predict the film temperature for a particular velocity at which the initial fouling would happen, i.e., threshold point. The results suggested that there would be zero or negligible fouling if the film temperature was maintained below the threshold value [41]. They employed the same concept of the competing mechanism of deposition and suppression as Kern and Seaton [28] suggested, which were modified to become independent of film thickness. The following equation presented the initial fouling rate.

$$\frac{dR_f}{dt} = \alpha Re^{-\beta} \exp(-E/RT_f) - \gamma \tau_w \quad (3)$$

where  $E$ , “ $\alpha$ ”, “ $\beta$ ”, and “ $\gamma$ ” are estimated from regression analysis of experimental data. By taking the left-hand side of Equation (3) equal to zero, one can easily develop a plot which relates the threshold film temperatures to the corresponding velocities (i.e., wall shear stress). This is useful to predict the threshold film temperature for a particular crude oil [40].

Many researchers modified this model to enhance its predictability for different crude oils and operating conditions. Panchal et al. [42] modified Ebert and Panchal’s model to improve its predictability for different experimental data sets by incorporating the Prandtl number in the deposition term. Using the usual heat transfer correlations, they assumed the power of 0.33 to the Prandtl number. Polley et al. [37] criticized the model by Panchal et al. because it predicted a more pronounced effect of velocity on threshold film temperature compared with experimental data from Knudsen et al. [43]. They modified the model in three aspects by (i) replacing film temperature with surface temperature, (ii) replacing the power of Reynolds number to  $-0.88$  from  $-0.66$  to justify for the turbulent flow in the tubes, and (iii) replacing the shear stress with  $Re^{0.8}$  in the removal term to characterize the controlling mechanism depending on mass transfer rather than shear stress as suggested by Crittenden [44]. The model showed good predictions of experimental data from Knudsen et al. and Ebert and Panchal with adjustment of the activation energy. Yeap et al. [45] modified the Epstein’s model [30] by introducing the suppression term. The suppression term was related to the mass transfer term for turbulent conditions. Although the model showed better predictability of Panchal, Knudsen’s lab data, and data from refineries, it requires more data for regression than previous models as it contains many fitting parameters. The model featured velocity dependencies in both the fouling deposition and suppression terms. It predicted well the behavior of maximum velocity in the initial fouling rate-velocity relationship shown by Crittenden et al. [31]. Nasr and Givi [46] modified the Polley’s model by removing the Prandtl number from the deposition term and changing the power of Reynolds number to 0.4 in the removal term. While the results predicted well the experimental data of Saleh et al. [47], the values of model parameters were more empirical, rendering its application to limited operating conditions.

Similarly, a slightly more empirical model was proposed by Shetty et al. [48]. They used the modified effective temperature instead of film temperature in Panchal’s models, which weighed more on bulk temperature than surface temperature. The model could successfully predict fouling at different velocities and bulk and surface temperatures for different crude oils. It also captured the decreasing fouling rate with increasing bulk temperatures due to the dissolution of fouling precursors. However, the effect of bulk temperature on fouling rate is still debatable due to contradictions in the experimental results [47,49]. Polley et al. [50] developed a semi-empirical model by eliminating the removal term from the threshold model and multiplying the deposition term with sticking probability ( $B$ ) as follows:

$$dR_f/dt = \alpha \exp(-E/RT_f)B \quad (4)$$

where  $A$  is the model fitting parameter which mainly depends on the crude oil composition. They assumed  $B$  to be a function of shear stress, which is 1 at low and 0 at high shear stress values, as it dictates the foulant particles transfer and residence time on the deposition surface. The sticking probability is related to shear stress as follows:

$$B = 1 - \left( \frac{\tau_w - 2}{98} \right)^{0.5} \quad (5)$$

The model produced an excellent fit for heat exchangers’ plant data, and it requires fewer fitting parameters than Ebert and Panchal’s model. There has been a tremendous effort to increase the predictability of threshold fouling models for different operating conditions and crude oil types. Still, it has not been achieved because of the complexity of the fouling mechanism. It can be employed in designing a heat exchanger by limiting the criteria, which ensures a long run of operation with zero or minimum fouling and

eliminates the need for cleaning. The basic assumptions behind the threshold model led to the following aspects of its utilization:

1. To predict the corresponding threshold film temperature at a certain velocity using the threshold curve;
2. To predict the initial fouling rate for a combination of different velocities and film temperatures.

The concept of the threshold model was mainly attributed to the initial growth of the fouling layer, i.e., the initial linear fouling rate. Thus, the fouling behavior might change after the onset of the initial fouling layer, which renders the application of the threshold model to fouling predictions inappropriate [37]. However, the model is adopted to predict the fouling on the already developed foulant layer [51]. This application utilizes the threshold model to estimate the fouling rates for corresponding velocities and changes in film temperature caused by varying thickness of the foulant layer. Polley et al. [52] and Ishiyama et al. [51,53], adopted a strategy to apply the threshold model for prediction of heat exchanger fouling by estimating the threshold model parameters using fouling resistance vs. time data from heat exchangers. This approach allowed them to predict the effect of variation in operating parameters on the fouling of a particular unit by employing the previous behavior with the same crude oil and to optimize the cleaning schedules. Coletti et al. [54] modified this strategy by directly using the temperatures and flow rates data to estimate model parameters. This scheme prevents the error introduced by assumptions in fouling resistance calculations, thus leading to accurate predictability of fouling behavior.

### 3.1. Significance of Activation Energy

Ebert and Panchal [40] suggested that higher activation energy indicates that the fouling is reaction dominant, but if physical processes are also involved, then it will decrease the temperature sensitivity of the process and ultimately result in lowered activation energy. Yeap et al. [45] pointed out that the temperature dependency of the deposition term in the threshold model should not be first-order because both the thermal conductivity and density of the fouling layer vary with temperature. They also assumed that a lower value of activation energy could indicate that physical processes are involved. On the contrary, less activation energy indicates a small threshold barrier for the reaction to occur and less temperature sensitivity, i.e., fouling is much associated with the reaction mechanism. Smith and Joshi [55] pointed out several limitations in using the reaction term in the deposition model, which are given as:

1. The activation energy term lost its validity in the fouling application because of various mechanisms involved with the chemical reaction. The value used for activation energy, which is merely a factor representing the combined effect of other factors such as the solubility of precursors, fluid velocity, mass transfer limitations, etc., misrepresent its true meaning. Using the data from Ebert and Panchal, they also showed that the activation energy value varied with velocity, demonstrating it to be not true activation energy;
2. The use of data fitting to estimate activation energy values from different fouling models gave different results for the same data set, as shown by Yeap et al. [45]. Also, the initial guess values in regression analysis affect the estimated parameter values. This makes activation energy no more than a fitting parameter, and dividing by gas constant in the exponential term should not have any significance;
3. Using reciprocal temperature in the exponential term can be replaced with normal temperature dependence because this term becomes linear at higher temperatures (i.e., crude oil fouling range). It was shown using the data from Ebert and Panchal [40] and Petkovic and Watkinson [56] that using normal temperature in the Arrhenius plot could also give a good fitting of the data;

4. The value of the exponential term decreases with increasing activation energy. Therefore, high activation energy values correspond to less contribution of the reaction term, as opposed to that suggested by Ebert and Panchal [40] and Yeap et al. [45].

Deshannavar and Ramasamy [57] modified the Panchal et al. [42] model using the idea of Smith and Joshi [55] by replacing the  $E_a/R$  ratio in the deposition term with a temperature-dependent constant  $G$ , which is defined as follows:

$$G = G_0 + \psi T_b \quad (6)$$

They showed that this model could represent the effect of bulk temperature on fouling rate, as demonstrated by Shetty et al. [48]. The proposed equation was given as

$$\frac{dR_f}{dt} = \alpha Re^{-\beta} Pr^{-0.33} \exp\left(\frac{-G}{T_f}\right) - \gamma \tau_w \quad (7)$$

The model was compared with the experimental data from different studies and predicted the fouling rates well. The model seems to show a simpler version of the previous threshold models, which removed the cumbersome activation energy term, but still, it relies on more fitting parameters such as  $\psi$  and  $G_0$  which would require additional experimental work to analyze the effect of bulk temperature on the fouling rate. The value of  $e$  represents the tendency of the fouling rate to be influenced by bulk temperature, which may result from fouling precursor solubility or asphaltene precipitation. However, there is still no evidence to ascertain whether the fouling was dominated by chemical reaction or particle deposition. Deshannavar and Ramasamy [57] assumed that if the fouling rate decreases with increasing bulk temperature, then asphaltene deposition is the dominant mechanism. However, Srinivasan [46] showed contradicting results with high asphaltene content in crude oil.

### 3.2. Prediction of Induction Period

While most of the proposed models predict the threshold point, which indicates that the fouling layer has already been formed, none described the induction period during which foulant is deposited on the clean surface. Yang et al. [58] proposed a model that describes the fouling during the induction (pre-conditioning) period from the start of deposition on a clean surface to the linear initial fouling rate. The model defined fractional surface coverage ( $\theta$ ) as proportional to the fouling growth rate. They assumed that during the induction period, the fouling rate ( $R'_f$ ) is constant, hence the overall fouling rate could be defined as

$$dR_f/dt = \theta R'_f \quad (8)$$

where the rate of surface coverage was related with time using a sigmoidal function as

$$\theta = \frac{k_1 - k_2}{k_1} \frac{1}{1 + w \exp(-(k_1 - k_2)t)} \quad (9)$$

where  $k_1$  and  $k_2$  are the deposition and removal constants, while  $w$  is the wettability parameter of the surface. The model also predicted well the length of the induction period, i.e., the time required to reach 50% of the maximum surface coverage [ $\theta_{t0.5} = 0.5 \times \theta_{\max}$ ]. A good fit of data was obtained for both organic and inorganic deposition at different surface temperatures and velocities. They also concluded that higher surface roughness would lead to shorter induction periods. They described that if  $k_2$  remains close to  $k_1$  by increasing the velocity, the actual fouling rate will be less than the predicted rate because the maximum surface coverage will be less than 1. For the first time, this model gave a significant mathematical description for physical phenomena related to induction periods. The validity of this approach could also be examined on the fouling behavior beyond the induction period where an asymptotic curve is formed corresponding to constant fouling resistance. The list of threshold fouling models is presented chronologically in Table 2.

**Table 2.** List of threshold fouling models in chronological order.

Model	Author (s), Year & Ref.	Fluid	Operating Parameters	Equipment	Notes
$dR_f/dt = \alpha Re^\beta \exp(-E/RT_f) - \gamma \tau_w$	Ebert & Panchal, 1995 [40]	Crude oil	$T_b = 505$ K $T_f = 643$ – $673$ K $u = 1.2$ – $5.2$ m/s	Heated tube	Introduced concept of fouling threshold condition.
$dR_f/dt = \alpha Re^{-0.66} Pr^{-0.33} \exp(-E/RT_f) - \gamma \tau_w$	Panchal et al., 1997 [42]	Crude oil	$T_b = 477$ – $636$ K $T_s = 505$ – $740$ K $u = 0.9$ – $3.2$ m/s	Heat exchanger, annular flow	Introduced effect of thermal conductivity and specific heat of crude oil.
$dR_f/dt = \alpha Re^{-0.8} Pr^{-0.33} \exp(-E/RT_s) - \gamma Re^{0.8}$	Polley et al., 2002 [37]	Crude oil	$T_b = 422$ – $477$ K $T_s = 477$ – $602$ K $u = 0.91$ – $3.05$ m/s	Annular flow	Replaced film temperature by surface temperature. Related removal term to mass transfer of turbulence.
$\frac{dR_f}{dt} = \frac{A_1 f u T_s^{2/3} \rho^{2/3} \mu^{-4/3}}{1 + A_2 u^3 f^2 \rho^{-1/3} \mu^{-1/3} T_s^{2/3} \exp(\frac{E}{RT_s})} - A_3 u^{0.8}$	Yeap et al., 2004 [45]	Crude oil	$T_s = 380$ – $593$ K $u = 0.63$ – $3.94$ m/s	Heat exchanger	
$dR_f/dt = \alpha Re^\beta \exp(-E/RT_f) - \gamma Re^{0.4}$	Nasr and Givi, 2006 [46]	Crude oil	$T_b = 353$ – $393$ K $T_s = 453$ – $518$ K $u = 0.25$ – $0.4$ m/s	Annular flow	Proposed model independent of Prandtl number.
$dR_f/dt = \alpha \exp(-E/RT_f) B$	Polley, 2010 [50]	Crude oil	N/A	Heat exchanger	Fewer fitting parameters than Ebert & Panchal's model
$dR_f/dt = \alpha Re^\beta Pr^{-0.33} \exp(-E/RT_{eff}) - \gamma \tau_w$	Shetty et al., 2016 [48]	Crude oil	$T_b = 355$ – $453$ K $T_s = 516$ – $607$ K $u = 0.35$ – $0.5$ m/s	Annular flow	Incorporate the effect of dissolution of precursor with increasing bulk temperature.
$dR_f/dt = \alpha Re^{-\beta} Pr^{-0.33} \exp(-G/T_f) - \gamma \tau_w$	Deshannavar & Ramasamy, 2020 [57]	Crude oil	$T_b = 353$ – $393$ K $T_s = 451$ – $499$ K $u = 0.4$ – $0.5$ m/s	Annular flow	Replace activation energy with temperature-dependent constant, G.

#### 4. Incorporation of Crude Stability/Compatibility

Asphaltenes have been associated as a primary precursor for crude oil fouling in crude preheat trains [59]. They are defined as the constituent of crude oil, which is insoluble in light paraffins such as n-pentane or n-heptane. They are considered the heaviest and highly polar molecules present in crude oils consisting of complex molecular structures that contain aromatic and naphthenic cores with alkyl side chains [60]. The presence of heteroatoms such as nitrogen, oxygen and sulfur increase these molecules' polarity, which results in agglomeration and deposition at the hot surface [61].

The stability of crude oil is its ability to maintain asphaltenes in a soluble state and not precipitate. In contrast, compatibility is the characteristic of a blend of crude oils due to which flocculation or precipitation of asphaltenes does not occur. Because crude oils themselves can be viewed as mixtures of different fractions, they sometimes become self-incompatible when their fractions are not compatible and induce asphaltenes precipitation [62]. Asomaning and Watkinson [63] found that fouling was controlled by asphaltenes solubility in crude oil at moderate temperatures, which was reflected by the increasing concentration of insoluble particles with crude oil instability. Wiehe [64] carried out fouling tests on different crude blends. It was demonstrated that asphaltenes precipitation could also be caused by nearly incompatible blends. Although the experimental data was very limited, but the blends with values of the ratio of solubility blending number and insolubility number ( $S_{BN}/I_N$ ) close to 1 showed asphaltenes deposition on a lab scale coking unit. Stark and Asomaning [59] estimated asphaltenes stability index (ASI) for different crude oil blends. They observed that blending heavy crude oil with light paraffinic oil led to asphaltenes' insolubility and caused high fouling in refinery preheat trains. They observed no effect of blending ratios on fouling behavior of an incompatible blend made by mixing high to low fouling potential crude. Saleh et al. [65] investigated the effects of blending crude oils using an annular HTRI probe. They showed that the initial fouling rate depends highly upon the proportions of crude oils blended. While data for solubility blending number was scattered, colloidal instability index (CII) was found to be the preferred parameter to relate with initial fouling rate. The results showed a linear relationship on a log-log plot between CII and the initial fouling rate. The proposed correlation was as follows:

$$\frac{dR_f}{dt} = 2.17 \times 10^{-9} \text{ CII}^{3.2} \quad (10)$$

Watkinson [5] demonstrated that fouling rates of crude blends were decreased with increasing velocity showing the adhesion process dominated over the transport process of the particles to the heat transfer surface. The strong dependency of fouling on temperature also confirmed that the adhesion or reaction process governed the fouling process. They also found that asphaltenes precipitation was dominant for heavy blends, while for light blends, suspended particles governed fouling. Hong and Watkinson [66] showed that aliphatic diluents promoted more fouling than aromatic diluents. They concluded that either the CII or the precipitation driving force [ $\delta_{\text{mix}} - \delta_f$ ] can be correlated with initial fouling rate with a difficult experimental procedure for the latter. Rogel et al. [20] tested different blends on the annular heating probe to develop a mathematical relationship between blend compatibility and fouling propensity, which is the temperature difference between the outlet temperature of oil at the end of the fouling test section and heater temperature of the fouling section. As fouling progresses, the fouling propensity will increase over time. It was observed that fouling propensity decreased with increasing compatibility of crude. They suggested that blend stability cannot be generalized to predict fouling of all crude blends because of variation in the inorganic content of different crude oils; however, stability of blends plays a significant role in optimization of concentration for specific blends only. They also found that deposits produced by compatible blends contain relatively high inorganic content when compared with less compatible blends. They

proposed an empirical model that relates blend compatibility parameters and inorganic content (ash) of crude oil with fouling propensity ( $\Delta T$ ), which is given as

$$\Delta T = 18.684 \log [(x_{ASP}/x_{ASH})(FR_{max}/(FR_{max} + P_o - 2(FR_{max}P_o)^{0.5}))] - 12.565 \quad (11)$$

A recent study [67] found that deposit removal by diffusion was decreased with solvent power of blend, which is demonstrated by high fouling resistance for less stable blends. The proposed empirical model was not capable of predicting fouling propensity for longer test runs due to the recirculation of crude oil and the ageing of the deposit. However, compatibility of blends showed a strong correlation with fouling propensity. Patil et al. [22] studied the effect of fouling by crude blends on the thermal and hydraulic performance of industrial preheat trains. They found the fouling propensity index (FPI) developed by Ho [68] to be an essential factor in fouling prediction by crude blends.

### 5. Effect of Ageing

Ageing refers to the transformation of deposits on the heat transfer surface from a gel to a coke-like material. It has a significant impact on heat exchangers' thermal and hydraulic performance [69]. This transformation is manifested as the change in thermal conductivity of the deposit from 0.2 to 1 W/m K [70]. Relying only on thermal performance could lead to the wrong estimation of fouling deposit composition and thickness. The change in heat transfer coefficient could also be related to the ageing of the deposit layer and pressure drop due to decreasing flow area during fouling layer growth.

Chunangad et al. [71] showed a good fit of pressure drop and temperature data by coupling the threshold model parameters and foulant thermal conductivity using a dynamic thermohydraulic model. Ishiyama et al. [69,72] developed the first ageing model using the experimental work from Fan and Watkinson [73]. They assumed that ageing is related to the chemical decomposition of the deposit with a decrease in the H/C ratio. To represent the process of deposit ageing, they also used youth factor  $y$ , which decreases from 1 to 0 as the coking of the deposit proceeds. The thermal conductivity of the deposit,  $\lambda_f$ , is represented as

$$\lambda_f = \lambda_F^\infty + (\lambda_F^o - \lambda_F^\infty)y \quad (12)$$

where  $\lambda_f^o$  and  $\lambda_f^\infty$  are the thermal conductivities of the deposit before and after ageing, respectively. The temperature dependency of the youth factor was modeled using the first-order kinetics. They assumed a thin slab approximation to measure the thickness of the deposited layer, i.e.,

$$\left. \frac{dx}{dt} \right|_i = \lambda_F^o \left( \frac{dR_f}{dt} \right) \quad (13)$$

where  $\left. \frac{dx}{dt} \right|_i$  is the growth rate of  $i$ th deposit sublayer, and  $\frac{dR_f}{dt}$  is the fouling rate at the deposit surface. They assumed that the thickness of the individual sublayer does not change, but its thermal conductivity will increase as modeled by Equation (12). The overall fouling resistance was calculated by summing the resistances of the individual sublayers.

$$R_f = \sum_{i=1}^n \frac{x_i}{\lambda_{F,i}} \quad (14)$$

They compared two modes of operation: constant wall temperature and constant heat flux. The former is usually practiced in laboratory equipment, while the latter is carried out in industrial heat exchangers [74]. The results suggested that for constant wall temperature operations, ageing promotes the deposition but reduces the thermal effect of fouling, leading to a faster increase in hydraulic resistance than thermal resistance. In constant heat flux operations, the ageing makes the fouling vary from asymptotic to linear behavior as it becomes faster. It shows that, with slow ageing, deposit removal has a significant effect on the fouling mechanism. Other studies [53,75] also showed that higher operating tem-

perature led to deposits with higher thermal conductivity. Coletti et al. [54,76], proposed a modified form of the previous model by Ishiyama et al. [72], which includes the variation in local conditions, making it a spatially distributed model. They employed cylindrical coordinates to overcome the limitations of thin-slab approximation in the previous model, which wrongly estimates fouling resistance for higher values of deposit thickness. They assumed the fouling layer as a moving boundary that changes its position according to process conditions. The results showed that the fouling resistance was overestimated when no ageing was considered in the fouling model. Similarly, the asymptotic behavior of the  $R_f$ - $t$  profile was achieved by including the effect of reduction in cross-sectional area of the tube, which served to remove deposits by increasing the velocity.

## 6. Thermal-Hydraulic Relationship

Mostly, the tube side pressure drops are estimated in refineries with direct measurement of pressure differences across the tubes in heat exchanger [77]. The effect of deposition buildup is also manifested in flow rate changes and cause the throughput variation. The pressure drop across the tube can be expressed as

$$\Delta P = 4f \frac{L}{d} \left( \frac{\rho u^2}{2} \right) \quad (15)$$

In terms of mass flow rate this can be reduced to

$$\Delta P = C \frac{f}{d^5} \quad (16)$$

where  $C$  represents the constant value. For a constant fanning friction factor, the ratio of fouled pressure drop ( $\Delta P_f$ ) and clean pressure drop ( $\Delta P_c$ ) [45] is given as

$$\frac{\Delta P_f}{\Delta P_c} = \left( 1 - \frac{x}{d} \right)^{-5} \quad (17)$$

Using the above ratio, a TH- $\lambda$  plot was proposed by Bejarano et al. [78] to monitor thermal-hydraulic behavior of heat exchangers as shown in Figure 1.

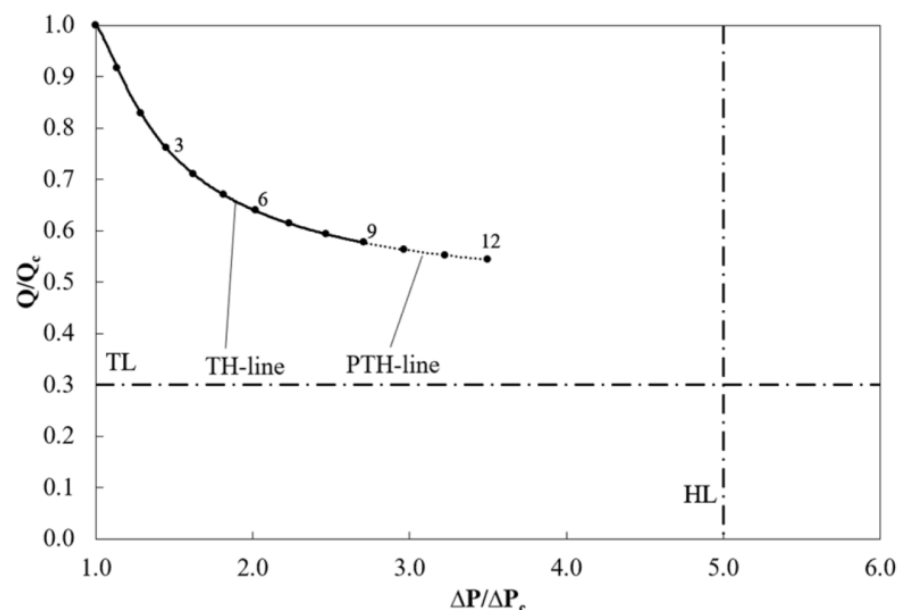


**Figure 1.** TH- $\lambda$  plot with TH and PTH lines. The dashed lines represent operating limits and dots represent the cleaning events. Reprinted with permission from Ref. [78], 2020, American Chemical Society.

The TH-line shown in the Figure 1 with solid line represents the performance of heat exchanger for nine months. The thermal effect on  $y$  axis represented by  $Q/Q_c$  which is the ratio of fouled and cleaned heat duties. The increase in pressure drop will be reflected by displacement along the  $x$  axis, while the thermal requirement is expressed in displacement in  $y$  direction. The TL and HL lines shows the allowable limits of operation such as maximum pressure drop or minimum heat duty. A predicted TH-line (PTH-line) can also be generated based on the thermal-hydraulic performance. This is very useful to predict future performance of heat exchanger and to highlight any variation in fouling mechanism.

The pressure drop measurements can be utilized to minimize the throughput loss when hydraulic limit of the operation is reached [78]. These pressure drop measurements along with thermal measurements can enhance the predictability of the fouling models. To form a relationship between these parameters a foulant Biot number ( $Bi$ ) based on a clean heat transfer coefficient ( $U_i$ ) is employed, which can be expressed as

$$Bi = R_f U_i \quad (18)$$

Using a thin slab approximation for constant mass flow rate and uniform deposition with constant friction factor, Equation (17) can be represented as

$$\frac{\Delta P_F}{\Delta P_c} = \left(1 - \frac{Bi}{Y}\right)^{-5} \quad (19)$$

where  $Y$  is the ratio of convective and conductive heat resistances [45] and expressed as

$$Y = \frac{dU_i}{\lambda_F} \quad (20)$$

For the deposition of foulant with varying roughness, Equation (19) can be represented as

$$\frac{\Delta P_F}{\Delta P_c} = \frac{f_F}{f_c} \left(1 - \frac{Bi}{Y}\right)^{-5} \quad (21)$$

where  $f_f$  and  $f_c$  represent the Fanning friction factor for foulant and clean tube. The thermal-hydraulic relationship in Equation (19) shows that deposition with higher surface roughness will decrease the heat transfer resistance accompanied by increased pressure drop [45]. This suggests the importance of pressure drop measurement along with thermal measurements for monitoring of fouling. It also indicates the error in foulant thickness estimation due to the roughness of the deposit layer. It is perceptible that the hydraulic effect will decrease with the value of  $Y$  and for values of  $Y$  less than 1, the fouling will increase the heat transfer, indicating foulant with very high thermal conductivity.

## 7. Role of Inorganic Content

Fouling has been associated mainly with asphaltenes deposition on heat transfer surfaces, but the inorganic content in crude oil substantially affects the overall fouling rate. It appears from the experimental studies that inorganic content can trigger the fouling of the organic species [11,42,79,80]. In many studies, the role of heteroatoms has been associated with the polarization of the organic molecules, which resulted in the formation of insoluble particles. On the other hand, the higher thermal conductivity of inorganic material (1–5 W/mK) is associated with lowering the thermal effect of fouling [81]. Mozdianfarid & Behranvand [82] found that 50% of the content of a fouling deposit in the industrial heat exchanger was inorganic material mainly containing iron and calcium compounds.

The most significant effect of inorganic content should manifest in the thermal conductivity of foulant. Bejarano et al. [83] modified the distributed model by incorporating the impact of inorganic content in thermal conductivity of a deposit ( $\lambda_L$ ). They assumed the threshold model for fouling and fixed relative proportions of both organic and inorganic material. The deposition and suppression constants ( $\alpha$  and  $\gamma$ ) were modified using the

weighted average thermal conductivity by using the mass fraction of organic and inorganic content as follows,

$$\lambda_F = w_{\text{org}}\lambda_{\text{org}} + w_{\text{inorg}}\lambda_{\text{inorg}} \quad (22)$$

$$\alpha' = \lambda_F a; \gamma' = \lambda_F \gamma \quad (23)$$

where  $w_{\text{org}}$  and  $w_{\text{inorg}}$  are mass fractions of organic and inorganic pseudo-components, respectively. The incorporation of inorganics improved the predictability of the model for refinery data. Bejarano et al. [13] developed a dynamic model with a moving boundary between the fouling layer and fluid. The varying thickness was related to deposition and removal mass fluxes, and the ageing of the deposit was represented by first-order chemical kinetics. The model allowed demonstration of the deposition of individual components, e.g., inorganics and organics, and includes the effect of blending and other operational instabilities on fouling. The organic deposition rate was assumed to be independent of inorganic content.

It has been found that both inorganic content and ageing affect heat exchangers' thermal and hydraulic performance [19]. The presence of inorganics and coke formation poses an error in the foulant thickness measurement due to the increased thermal conductivity of the deposit. The change in the heat transfer coefficient could also be related to the ageing of the deposited layer and decreasing flow area during the fouling layer growth. Thus, relying only on thermal performance could incorrectly estimate fouling deposit composition and thickness.

In subsequent studies, Bejarano et al. [80,84,85] assumed that inorganic deposition is related to organic deposition in terms of proportionality  $p_i$ , which is the ratio of inorganic to organic deposition rate and varies according to the oil contents, as

$$p_i = \frac{\phi_i / \rho_i}{\phi_{\text{ref}} / \rho_o} \quad (24)$$

They analyzed plant measurements to identify the evolution history of deposit thickness and its thermal conductivity. To account for the deposit with different proportions of organic and inorganic constituent, the variation in thermal conductivity with time was employed using various thermal conductivity mixing models. A good agreement was found with the deposit sample compositional analysis. The results of the fouling state analysis were used to predict the parameters of the fouling rate model. An excellent fit to plant data, especially acute fouling periods, was achieved when the mixed organic-inorganic deposition model incorporated the time-varying proportionality ratio. The deposition rate and thermal conductivity analysis confirmed that the deposition rate peaked at high inorganic content in the deposition layer. They also added the reinforcing parameter ( $p_{i/o}$ ), which represents the promotion of organic deposition by inorganic deposition, in the deposition rate model as shown in Equation (18). The value of  $p_{i/o}$  was found to be 0.24.

$$\phi_{\text{inorg}} = \frac{\phi_{\text{ref}} + p_{i/o} \rho_{\text{org}} \phi_{\text{F,inorg}}}{\rho_{\text{inorg}}} \quad (25)$$

## 8. CFD Simulations

In recent years, CFD simulations have been a powerful tool among researchers to identify the fouling behavior that is less costly and time consuming than it would be using the experimental means. It has also provided the freedom to use different geometries, compositions, and operating conditions, which would be tedious if done at a lab scale [25]. A significant aspect of CFD modeling is identifying the critical areas in the geometry which are mostly affected by fouling [86]. Brahma et al. [87] simulated a crystallization fouling on a heat transfer surface in an annular channel. They compared different surface structures affecting the fouling behavior.

The thermodynamics aspect of fouling has been neglected in heat exchanger applications. The thermodynamic models can well describe the asphaltenes precipitation phenomenon. Svendsen [88] developed a thermodynamic model for wax deposition in oil pipelines by describing a solid-liquid equilibrium state based on the activity coefficients. Sileri et al. [89] simulated asphaltenes deposition by adopting the Svendsen model. They quantified the mass of precipitated asphaltenes and its diffusion to the surface. They also incorporated the ageing by applying the rheological model, which characterizes the change of viscosity of the deposit with time. In the ageing model, the structuration and destructuration of foulant were related to time and shear rate, respectively. Yang et al. [90] simulated foulant ageing in terms of change in thermal conductivity and viscosity. They assumed an initially deposited layer of foulant, which eliminates the induction period calculation. Although the results were not validated with experimental data, they depicted the foulant removal and ageing phenomena well.

The CFD tool also provides the freedom to analyze various fouling models independently. Yang et al. [91] examined the relationship between two routes of fouling, namely chemical reaction, and asphaltenes precipitation. They simulated both models in a CFD study to compare fouling by the individual or combined route. It was reported that asphaltenes deposition by reaction route was seven to eight times more than the precipitation route. They also observed that reaction fouling increases with increased heat transfer due to the high thermal conductivity fouling layer, while the temperature gradient near the wall promoted precipitation fouling caused by the formation of hot spots. It was found that the reaction route fouling was prompted at the expense of precipitation fouling.

Most CFD studies used the Arrhenius law to define chemical reaction fouling which provides a more straightforward description of the fouling mechanism when compared with semi-empirical models. Bayat et al. [92] simulated a heat exchanger pipe model to predict the fouling rate using the Arrhenius kinetic model. They assumed arbitrary values for diffusion coefficients of pseudo components. The model over-predicted the induction period, which is opposed to the concept of threshold point in fouling rate. The effect of ageing and pressure drop was not incorporated into the model, which annulled its applicability to hydraulic limitations because of fouling. Yang et al. [93,94] found that the shear stress has a crucial role in defining the suppression term in the fouling prediction model, especially when predicting the fouling threshold point. They suggested not using the fouling prediction model directly for complex geometries because of the difference in shear stress. They also studied the effect of tube inserts in three-dimensional geometry and found that the heat transfer coefficient was enhanced compared with bare tube geometry. They also identified a low shear region behind the edge of the tube insert where the local wall temperature was high and susceptible to a high fouling rate.

CFD can be advantageously used as a prediction tool for the estimation of distributed fouling characteristics by combining the thermohydraulic numerical simulation with threshold fouling model. These dynamic models can provide real time information on the foulant thickness, removal rate, and ageing of the deposits. In a CFD analysis of a single heat exchanger, Chambon et al. [95] found that the average local fouling rate from a simulation was comparable to the overall fouling rate calculated using average input parameters such as Reynolds number, film temperature, and shear stress values. They employed discretization of operating parameters to estimate local fouling rates in a numerical simulation of a dynamic threshold fouling model. They observed little effect of thermohydraulic parameters on the deposition rate which is mainly controlled by the fouling rate. A great benefit that has been provided by the CFD tool is to carry out the parametric study [15]. Haghshenasfard et al. [96] simulated the asphaltenes deposition rate and compared the effect with varying velocity, surface roughness, temperature, and asphaltenes concentration. Asphaltenes deposition was simulated by applying a mass transfer model, and a simple kinetic model was adopted for surface reactions. Good agreement was achieved for validation with experimental data. However, the model does not contain the deposition removal term, and the flow was not considered fully developed. Emani et al. [97] simulated

the crude oil fouling in a single heat exchanger tube by assuming the crude oil as a mixture of pseudo components such as petroleum, asphaltenes, and salt. The multiphase mass transfer model was adopted for species transport. Two cases of wall shear stress were compared to analyze the effect on fouling, namely no-slip boundary (zero velocity at the wall) and wall shear stress boundary. The simulation results suggested that the shear stress boundary condition induced lesser fouling, which depicts the removal of deposits by the fluid turbulence at the wall.

In another study, Emani et al. [98] adopted a Eulerian-Lagrangian approach to simulate the asphaltenes deposition. The asphaltenes were considered a discrete phase distributed in the continuous phase of crude oil. The particle deposition and removal were modeled using thermophoretic force and Saffman lift force models, respectively. They found that asphaltenes deposition increased with particle size. Contrary to the definition of thermophoretic force, which is directly proportional to the temperature gradient [99], the results showed that particle deposition increased with the temperature gradient.

Most of the simulation studies assumed a constant wall thickness with varying properties. Paz et al. [100] used a moving boundary approach to simulate the fouling deposition by exhaust gases. They employed the dynamic mesh tool to demonstrate the increase in fouling layer thickness. The dynamic mesh could reproduce the movement of the foulant-fluid interface with increasing thickness. This method can help predict the pressure drop caused by a reduced cross-sectional area due to fouling.

## 9. Conclusions

Since the development of Kern's model, a great effort has been put into developing a robust and efficient fouling model to encompass the various aspects of the fouling mechanism, such as applicability to wide operating conditions, diverse crude oil composition, and ageing of the deposit. Although the complex composition of crude oil is still the biggest hurdle to predicting the exact fouling rate, these efforts have shown considerable progress in the past decade. Various aspects in the development of fouling modeling have been reviewed. The main points are summarized as:

1. Using both deposition and removal terms in fouling models is criticized due to multiple empirical parameters involved. Models containing the removal parameter within the deposition term have shown comparable results and reduced fitting parameters. The removal term is highly susceptible to flow behavior, which is related to flow geometry; this emphasizes the need for a conversion factor when comparing experimental data from different geometries;
2. The inclusion of the asymptotic surface coverage model is a promising approach in predicting the induction periods by combining with the fouling model to achieve a comprehensive model for longer duration;
3. The activation energy in the Ebert and Panchal model has lost its validity in the Arrhenius deposition term as its value is affected by the physical processes. A better way to describe the deposition term is to introduce parameter for temperature dependency of the crude oil properties;
4. The rate of asphaltenes precipitation reaction has been neglected as part of the deposition model, despite the increasing demand of opportunity crudes and blending operation. The colloidal instability parameters seem promising to incorporate in the deposition model, despite the complex dependency of asphaltenes precipitation on crude oil temperature and composition. A more practical approach would be to find the relationship between the deposition constant and the instability parameter of the crude oil or blend;
5. Foulant ageing and the presence of inorganic content can cause errors in estimating the thickness of foulant layers due to an increase in foulant thermal conductivity. However, accurate prediction of fouling rate and foulant thickness can be achieved by incorporating ageing and mixing models for foulant thermal conductivity. In addition, the reduction in throughput loss near the hydraulic limit of the operation can be

achieved through pressure drop measurements. Therefore, relying solely on thermal performance could lead to inaccurate estimations of fouling rate and thickness of foulant. It is, therefore, recommended to include the hydraulic performance data as necessary tool to evaluate the fouling behavior of heat exchangers;

6. With difficulty in data acquisition and the long duration of experimental studies, CFD simulations can play a critical role in assessing the application of different models with a wide range of operating conditions and geometries. The application of dynamic mesh needs to be further explored to capture accurate hydraulic performance.

**Author Contributions:** Ideation, O.u.R. and M.G.R.; resources, O.u.R., M.G.R., N.E.M.R., S.M.; data curation, A.S.M.G. and A.H.Q.; writing—original draft preparation, O.u.R.; writing—review and editing, M.G.R., N.E.M.R., S.M., A.S.M.G. and A.H.Q.; funding acquisition, M.G.R. and N.E.M.R. All authors have read and agreed to the published version of the manuscript.

**Funding:** This research was funded by Yayasan UTP, grant No. 015LC0-130.

**Data Availability Statement:** No new data were created or analyzed in this study. Data sharing is not applicable to this article.

**Acknowledgments:** The authors gratefully acknowledge Chemical Engineering Department, Universiti Teknologi PETRONAS, Malaysia for providing adequate facilities throughout this study.

**Conflicts of Interest:** The authors declare no conflict of interest.

## Nomenclature

A	Arrhenius coefficient
$A_{1-3}$	Model constants
B	Sticking Probability
Bi	Biot number
c	Concentration of foulants, $\text{kg}/\text{m}^3$
$c_i$	Concentration of foulants at $i^{\text{th}}$ site, $\text{mol}/\text{m}^3$
$c_{t,0}$	total number of sites at $t=0$ , $\text{mol}/\text{m}^2$
$c_{A,S}$	sites occupied by A, $\text{mol}/\text{m}^2$
$c_{AS}$	concentration of A on the surface, $\text{mol}/\text{m}^2$
CII	Colloidal instability index
d	tube inner diameter, m
E	Activation energy, J/mol
e	Roughness, m
f	fanning friction factor
$FR_{\text{max}}$	maximum flocculation ratio
G	Temperature-dependent constant, K
$G_o$	Model parameter, K
J	mass deposition rate, $\text{kg}/\text{s}$
$k_1, k_2$	lumped rate constants, $\text{s}^{-1}$
$k_m$	deposition constant, $\text{m}^4/\text{kg}^2$
$k_r$	removal constant, $\text{m}^2/\text{N s}$
L	tube length, m
M	molar mass, $\text{kg}/\text{kmol}$
m	mass of deposit per unit surface area, $\text{kg}/\text{m}^2$
$\dot{m}_i$	mass flux, $\text{kg}/\text{m}^2 \text{ s}$
P	Pressure, Pa
$P_o$	Peptizing power of maltenes
Pr	Prandtl number
$p_i$	ratio of inorganic to organic deposition rate of component i
Q	Heat transfer rate, Watt
R	Gas constant, J/mol K
$R_f$	thermal resistance, $\text{m}^2\text{K}/\text{W}$
$R'_f$	rate of fouling, $\text{m}^2\text{K}/\text{J}$

Re	Reynolds number
$r_i$	initial rate of fouling reaction, $s^{-1}$
S	roughness parameter
$S_c$	Schmidt number
T	time, s
T	Temperature, K
U	Heat transfer coefficient, $W/m^2K$
u	mean flow velocity, m/s
w	wettability parameter
$w_i$	mass fraction of i component
x	deposit thickness, m
$x_{ASP}$	Asphaltenes content
$x_{ASH}$	Ash content
Y	Ratio of convective and conductive heat resistances
y	youth factor
<b>Greek</b>	
$\alpha$	model fitting parameter [Equations (3) and (9)], $K s^2/kg$
$\beta$	model fitting parameter, dimensionless
$\gamma$	model fitting parameter [Equations (3) and (9)], $m^3 K s/J kg$
$\Delta$	difference
$\theta$	fractional surface coverage
$\lambda$	thermal conductivity, $W/m K$
$\mu$	dynamic viscosity, $Pa s$
$\rho$	density, $kg/m^3$
$\tau$	shear stress, $N/m^2$
$\varnothing$	rate of deposition, $kg/m^2 s$
$\psi$	model fitting parameter, dimensionless
<b>Subscripts</b>	
b	Bulk fluid
c	crude oil
D	Deposition
eff	Effective
f	Film
F	Foulant
inorg	Inorganic component
org	Organic component
R	Removal
s	Surface
s0	Surface initial
w	Wall
<b>Superscripts</b>	
o	fresh deposit
$\infty$	aged deposit

## References

- Borges, J.L.; Queiroz, E.M.; Pessoa, F.L.P.; Liporace, F.S.; Oliveira, S.G.; Costa, A.L.H. Fouling management in crude oil preheat trains through stream split optimization. *Comput. Aided Chem. Eng.* **2009**, *27*, 1587–1592. [[CrossRef](#)]
- Dai, B.; Liu, C.; Liu, S.; Wang, D.; Wang, Q.; Zou, T.; Zhou, X. Life cycle techno-enviro-economic assessment of dual-temperature evaporation transcritical CO<sub>2</sub> high-temperature heat pump systems for industrial waste heat recovery. *Appl. Therm. Eng.* **2023**, *219*, 119570. [[CrossRef](#)]
- Van Nostrand, J.L.; Leach, W.L.J.; Haluska, S.H. Economic Penalties Associated with the Fouling of Refinery Heat transfer Equipment. In *Fouling of Heat Transfer Equipment*; Hemisphere Publishing: New York, NY, USA, 1981; pp. 619–643.
- Coletti, F.; Hewitt, G.F. *Crude Oil Fouling Deposit Characterization, Measurements, and Modeling*; Gulf Professional Publishing: Oxford, UK, 2015.
- Watkinson, A.P. Deposition from Crude Oils in Heat Exchangers. *Heat Transf. Eng.* **2007**, *28*, 177–184. [[CrossRef](#)]
- Müller-Steinhagen, H.; Malayeri, M.R.; Watkinson, A.P. Heat Exchanger Fouling: Environmental Impacts. *Heat Transf. Eng.* **2009**, *30*, 773–776. [[CrossRef](#)]

7. Coletti, F.; Macchietto, S. Predicting refinery energy losses due to fouling in heat exchangers. *Comput. Aided Chem. Eng.* **2009**, *27*, 219–224. [[CrossRef](#)]
8. Costa, A.L.H.; Tavares VB, G.; Borges, J.L.; Queiroz, E.M.; Pessoa FL, P.; Liporace FD, S.; de Oliveira, S.G. Parameter estimation of fouling models in crude preheat trains. *Heat Transf. Eng.* **2013**, *34*, 683–691. [[CrossRef](#)]
9. Dickakian, S.; Seay, G.B. Asphaltene precipitation primary crude exchanger fouling mechanism. *Oil Gas J.* **1988**, *86*, 47–50.
10. Watkinson, A.P.; Wilson, D.I. Chemical reaction fouling: A review. *Exp. Therm. Fluid Sci.* **1997**, *14*, 361–374. [[CrossRef](#)]
11. Smith, A.D.; Ishiyama, E.M.; Harris, J.; Lane, M. Translating Crude Oil Fouling Testing Rig Data To The Field: A Road Map For Future Research. In Proceedings of the International Conference on Heat Exchanger Fouling and Cleaning XII, Aranjuez, Spain, 11–16 June 2017.
12. Wilson, D.I.; Ishiyama, E.M.; Polley, G.T. Twenty Years of Ebert and Panchal—What Next? *Heat Transf. Eng.* **2017**, *38*, 669–680. [[CrossRef](#)]
13. Diaz-Bejarano, E.; Coletti, F.; Macchietto, S. A New Dynamic Model of Crude Oil Fouling Deposits and Its Application to the Simulation of Fouling-Cleaning Cycles. *AIChE J.* **2016**, *62*, 90–107. [[CrossRef](#)]
14. Diaz-Bejarano, E.; Coletti, F.; Macchietto, S. Thermo-hydraulic analysis of refinery heat exchangers undergoing fouling. *AIChE J.* **2017**, *63*, 984–1001. [[CrossRef](#)]
15. Maddahian, R.; Farsani, A.T.; Ghorbani, M. Numerical investigation of asphaltene fouling growth in crude oil preheat trains using multi-fluid approach. *J. Pet. Sci. Eng.* **2020**, *188*, 106879. [[CrossRef](#)]
16. Salimi, F.; Ayatollahi, S.; Seftie, M.V. Prediction of asphaltene deposition during turbulent flow using heat transfer approach. *Pet. Sci. Technol.* **2018**, *36*, 632–639. [[CrossRef](#)]
17. Diaz-Bejarano, E.; Coletti, F.; Macchietto, S. Complex crude oil fouling layers: Use of model predictions to detect inorganics breakthrough. *Appl. Therm. Eng.* **2018**, *141*, 666–674. [[CrossRef](#)]
18. Rammerstorfer, E.; Karner, T.; Siebenhofer, M. The kinetics and mechanisms of fouling in crude oil heat transfer. *Heat Transf. Eng.* **2019**, *41*, 691–707. [[CrossRef](#)]
19. Coletti, F.; Macchietto, S.; Diaz-Bejarano, E. Beyond Fouling Factors: A Reaction Engineering Approach to Crude Oil Fouling Modelling. In Proceedings of the International Conference on Heat Exchanger Fouling and Cleaning XI, Enfield, Ireland, 7–12 June 2015; pp. 89–96.
20. Rogel, E.; Hench, K.; Miao, T.; Lee, E.; Dickakian, G. Evaluation of the Compatibility of Crude Oil Blends and Its Impact on Fouling. *Energy Fuels* **2018**, *32*, 9233–9242. [[CrossRef](#)]
21. Kumar, R.; Voolapalli, R.K.; Upadhyayula, S. Prediction of crude oil blends compatibility and blend optimization for increasing heavy oil processing. *Fuel Process. Technol.* **2018**, *177*, 309–327. [[CrossRef](#)]
22. Patil, P.D.; Kozminski, M.; Peterson, J.; Kumar, S. Fouling Diagnosis of Pennsylvania Grade Crude Blended with Opportunity Crude Oils in a Refinery Crude Unit's Hot Heat Exchanger Train. *Ind. Eng. Chem. Res.* **2019**, *58*, 17918–17927. [[CrossRef](#)]
23. Ogbonnaya, S.; Ajayi, O. Fouling phenomenon and its effect on heat exchanger: A review. *Front. Heat Mass Transf.* **2017**, *9*, 31. [[CrossRef](#)]
24. Wang, Y.; Yuan, Z.; Liang, Y.; Xie, Y.; Chen, X.; Li, X. A review of experimental measurement and prediction models of crude oil fouling rate in crude refinery preheat trains. *Asia-Pac. J. Chem. Eng.* **2015**, *10*, 607–625. [[CrossRef](#)]
25. Müller-Steinhagen, H. Heat transfer fouling: 50 years after the Kern and Seaton model. *Heat Transf. Eng.* **2011**, *32*, 1–13. [[CrossRef](#)]
26. Deshannavar, U.; Rafeen, S.; Gounder, R.M.; Subbarao, D. Crude Oil Fouling: A Review. *J. Appl. Sci.* **2010**, *10*, 3167–3174. [[CrossRef](#)]
27. Wilson, D.I.; Polley, G.; Pugh, S. Ten Years of Ebert, Panchal and The 'Threshold Fouling' Concept. In Proceedings of the 6th International Conference on Heat Exchanger Fouling and Cleaning—Challenges and Opportunities, Kloster Irsee, Germany, 5–10 June 2005.
28. Kern, D.Q.; Seaton, R.E. A theoretical analysis of thermal surface fouling. *Br. Chem. Eng.* **1959**, *4*, 258–262.
29. Watkinson, A.P. Particulate Fouling of Sensible Heat Exchangers. Ph.D. Dissertation, The University of British Columbia, Vancouver, BC, USA, 1968.
30. Epstein, N. A Model of the Initial Chemical Reaction Fouling Rate for Flow within a Heated Tube and its Verification. In Proceedings of the International Heat Transfer Conference 10, Brighton, UK, 14–18 August 1994.
31. Crittenden, B.D.; Kolaczowski, S.T.; Takemoto, T.; Phillips, D.Z. Crude Oil Fouling in a Pilot-Scale Parallel Tube Apparatus. *Heat Transf. Eng.* **2009**, *30*, 777–785. [[CrossRef](#)]
32. Paterson, W.R.; Fryer, P.J. A reaction engineering approach to the analysis of fouling. *Chem. Eng. Sci.* **1988**, *43*, 1714–1717. [[CrossRef](#)]
33. Chambon, A.; Ratel, M.; Anxionnaz-Minvielle, Z.; Aquino, B.; Buffet, A.; Vinet, B. Fouling in the crude oil distillation preheat train: Comparison of experimental data with model results. In Proceedings of the International Conference on Heat Exchanger Fouling and Cleaning, Enfield, Ireland, 7–12 June 2015; pp. 74–80.
34. Joshi, H.M. Crude oil fouling field data and a model for pilot-plant scale data. In Proceedings of the International Conference on Heat Exchanger Fouling and Cleaning, Budapest, Hungary, 9–14 June 2013; pp. 22–26.
35. Watkinson, A.P. Deposition From Crude Oils In Heat Exchangers. In Proceedings of the Heat Exchanger Fouling and Cleaning—Challenges and Opportunities, Kloster Irsee, Germany, 5–10 June 2005.
36. Scarborough, C.E.; Cherrington, D.C.; Diener, R. Coking of crude oil at high heat flux levels. *Chem. Eng. Prog.* **1979**, *75*, 41–46.

37. Polley, G.T.; Wilson, D.I.; Yeap, B.L.; Pugh, S.J. Evaluation of laboratory crude oil threshold fouling data for application to refinery pre-heat trains. *Appl. Therm. Eng.* **2002**, *22*, 777–788. [[CrossRef](#)]
38. Yang, M.; O'meara, A.; Crittenden, B.D. Determination of Crude Oil Fouling Thresholds. In Proceedings of the International Conference on Heat Exchanger Fouling and Cleaning, Crete Island, Greece, 5–10 June 2011.
39. Crittenden, B.D.; Kolaczowski, S.T.; Downey, I.L. Fouling of crude oil preheat exchangers. *Chem. Eng. Res. Des.* **1992**, *70*, 547–557.
40. Ebert, W.; Panchal, C.B. Analysis of Exxon Crude-Oil-Slip Stream Coking Data. In *Fouling Mitigation of Industrial Exchange Equipment*; Begell House: New York, NY, USA, 1995; pp. 451–460.
41. Rodriguez, C.; Smith, R. Optimization of operating conditions for mitigating fouling in heat exchanger networks. *Chem. Eng. Res. Des.* **2007**, *85*, 839–851. [[CrossRef](#)]
42. Panchal, C.B.; Kuru, W.C.; Liao, C.F.; Ebert, W.A.; Palen, J.W. Threshold Conditions for Crude Oil Fouling. In *Understanding Heat Exchanger Fouling and Its Mitigation*; Engineering Foundation: New York, NY, USA, 1997; pp. 273–279.
43. Knudsen, J.G.; Dahcheng, L.; Ebert, W.A. The Determination of the Threshold Fouling Curve for a Crude Oil. In *Understanding Heat Exchanger Fouling and Its Mitigation*; Begell House: New York, NY, USA, 1999; pp. 265–272.
44. Crittenden, B.; Kolaczowski, S.T.; Hout, S.A. Modelling hydrocarbon fouling. *Chem. Eng. Res. Des.* **1987**, *65*, 171–179.
45. Yeap, B.L.; Wilson, D.I.; Polley, G.T.; Pugh, S.J. Mitigation of Crude Oil Refinery Heat Exchanger Fouling Through Retrofits Based on Thermo-Hydraulic Fouling Models. *Chem. Eng. Res. Des.* **2004**, *82*, 53–71. [[CrossRef](#)]
46. Nasr, M.R.J.; Givi, M.M. Modeling of crude oil fouling in preheat exchangers of refinery distillation units. *Appl. Therm. Eng.* **2006**, *26*, 1572–1577. [[CrossRef](#)]
47. Saleh, Z.S.; Sheikholeslami, R.; Watkinson, A.P. Fouling characteristics of a light Australian crude oil. *Heat Transf. Eng.* **2005**, *26*, 15–22. [[CrossRef](#)]
48. Shetty, N.; Deshannavar, U.B.; Marappagounder, R.; Pendyala, R. Improved threshold fouling models for crude oils. *Energy* **2016**, *111*, 453–467. [[CrossRef](#)]
49. Srinivasan, M.; Watkinson, A.P. Fouling of Some Canadian Crude Oils. *Heat Transf. Eng.* **2005**, *26*, 7–14. [[CrossRef](#)]
50. Polley, G.; Tamakloe, E.; Wilson, I.; Macchietto, S.; Coletti, F. Development of a model for the prediction of fouling in heat exchangers processing crude oil. In Proceedings of the 10AIChE–2010 AIChE Spring Meeting and 6th Global Congress on Process Safety, San Antonio, TX, USA, 21–25 March 2010.
51. Ishiyama, E.M.; Heins, A.V.; Paterson, W.R.; Spinelli, L.; Wilson, D.I. Scheduling cleaning in a crude oil preheat train subject to fouling: Incorporating desalter control. *Appl. Therm. Eng.* **2010**, *30*, 1852–1862. [[CrossRef](#)]
52. Polley, G.T.; Tamakloe, E.; Nunez, M.P.; Ishiyama, E.M.; Wilson, D.I. Applying thermo-hydraulic simulation and heat exchanger analysis to the retrofit of heat recovery systems. *Appl. Therm. Eng.* **2013**, *51*, 137–143. [[CrossRef](#)]
53. Ishiyama, E.M.; Pugh, S.J.; Wilson, D.I. Incorporating Deposit Ageing into Visualisation of Crude Oil Preheat Train Fouling. *Process Integr. Optim. Sustain.* **2020**, *4*, 187–200. [[CrossRef](#)]
54. Coletti, F.; Macchietto, S. A Dynamic, Distributed Model of Shell-and-Tube Heat Exchangers Undergoing Crude Oil Fouling. *Ind. Eng. Chem. Res.* **2011**, *50*, 4515–4533. [[CrossRef](#)]
55. Smith, A.D.; Joshi, H.M. A Critical Look at the Use of Activation Energy in Crude Oil Fouling Models. In Proceedings of the International Conference on Heat Exchanger Fouling and Cleaning, Enfield, Ireland, 7–12 June 2015.
56. Petkovic, B.; Watkinson, P. Fouling of a heated rod in a stirred tank system. *Heat Transf. Eng.* **2014**, *35*, 302–310. [[CrossRef](#)]
57. Deshannavar, U.B.; Marappagounder, R. Revisiting Threshold Fouling Models for Crude Oil Fouling. *Heat Transf. Eng.* **2020**, *42*, 1–17. [[CrossRef](#)]
58. Yang, M.; Young, A.; Niyetkaliyev, A.; Crittenden, B. Modelling fouling induction periods. *Int. J. Therm. Sci.* **2012**, *51*, 175–183. [[CrossRef](#)]
59. Stark, J.L.; Asomaning, S. Crude Oil Blending Effects on Asphaltene Stability in Refinery Fouling. *Pet. Sci. Technol.* **2003**, *21*, 569–579. [[CrossRef](#)]
60. Rashid, Z.; Wilfred, C.D.; Gnanasundaram, N.; Arunagiri, A.; Murugesan, T. A comprehensive review on the recent advances on the petroleum asphaltene aggregation. *J. Pet. Sci. Eng.* **2019**, *176*, 249–268. [[CrossRef](#)]
61. Rogel, E.; Roye, M.; Vien, J.; Miao, T. Characterization of Asphaltene Fractions: Distribution, Chemical Characteristics, and Solubility Behavior. *Energy Fuels* **2015**, *29*, 2143–2152. [[CrossRef](#)]
62. Gray, M.R.; Yarranton, H.W. Quantitative Modeling of Formation of Asphaltene Nanoaggregates. *Energy Fuels* **2019**, *33*, 8566–8575. [[CrossRef](#)]
63. Watkinson, S.A.A.P. Petroleum Stability and Heteroatom Species Effects in Fouling of Heat Exchangers by Asphaltenes. *Heat Transf. Eng.* **2000**, *21*, 10–16. [[CrossRef](#)]
64. Wiehe, I.A.; Kennedy, R.J.; Dickkian, G. Fouling of Nearly Incompatible Oils. *Energy Fuels* **2001**, *15*, 1057–1058. [[CrossRef](#)]
65. Saleh, Z.; Sheikholeslami, R.; Watkinson, P. Blending Effects on Fouling of Four Crude Oils. In Proceedings of the 6th International Conference on Heat Exchanger Fouling and Cleaning—Challenges and Opportunities, Kloster Irsee, Germany, 5–10 June 2005.
66. Hong, E.; Watkinson, A.P. Precipitation and Fouling in Heavy Oil-Diluent Blends. *Heat Transf. Eng.* **2009**, *30*, 786–793. [[CrossRef](#)]
67. Rogel, E.; Hench, K.; Cibotti, F.; Forbes, E.; Jackowski, L. Investigation on Crude Oil Fouling Behavior. *Energy Fuels* **2022**, *36*, 818–825. [[CrossRef](#)]
68. Ho, T.C. A study of crude oil fouling propensity. *Int. J. Heat Mass Transf.* **2016**, *95*, 62–68. [[CrossRef](#)]

69. Wilson, D.I.; Ishiyama, E.M.; Paterson, W.R.; Watkinson, A.P. Ageing: Looking backward and looking forward. In Proceedings of the International Conference on Heat Exchanger Fouling and Cleaning VIII—2009, Schlading, Austria, 14–19 June 2009; pp. 221–230.
70. Diaz-Bejarano, E.; Coletti, F.; Macchietto, S. Modeling and Prediction of Shell-Side Fouling in Shell-and-Tube Heat Exchangers. *Heat Transf. Eng.* **2019**, *40*, 845–861. [[CrossRef](#)]
71. Chunangad, K.S.; Chang, R.Y.; Casebolt, R.P. Evaluation and Prediction of the Thermal and Hydraulic Impact of Crude Oil Fouling on Exchanger Performance Using Pressure Measurements. In Proceedings of the Heat Exchanger Fouling and Cleaning, Aranjuez, Spain, 11–16 June 2017; pp. 1–4.
72. Ishiyama, E.A.; Coletti, F.; Macchietto, S.; Paterson, W.R.; Wilson, D.I. Impact of Deposit Ageing on Thermal Fouling: Lumped Parameter Model. *AIChE J.* **2009**, *56*, 531–545. [[CrossRef](#)]
73. Fan, Z.; Watkinson, A.P. Aging of Carbonaceous Deposits from Heavy Hydrocarbon Vapors. *Ind. Eng. Chem. Res.* **2006**, *45*, 6104–6110. [[CrossRef](#)]
74. Ishiyama, E.M.; Paterson, W.R.; Wilson, D.I. Exploration of alternative models for the aging of fouling deposits. *AIChE J.* **2011**, *57*, 3199–3209. [[CrossRef](#)]
75. Ishiyama, E.M.; Falkeman, E.; Wilson, D.I.; Pugh, S.J. Quantifying Implications of Deposit Aging from Crude Refinery Preheat Train Data. *Heat Transf. Eng.* **2020**, *41*, 115–126. [[CrossRef](#)]
76. Coletti, F.; Ishiyama, E.M.; Paterson, W.R.; Wilson, D.I.; Macchietto, S. Impact of Deposit Aging and Surface Roughness on Thermal Fouling: Distributed Model. *AIChE J.* **2010**, *56*, 3257–3273. [[CrossRef](#)]
77. Mozdianfard, M.R.; Behranvand, E. A field study of fouling in CDU preheaters at Esfahan refinery. *Appl. Therm. Eng.* **2013**, *50*, 908–917. [[CrossRef](#)]
78. Diaz-Bejarano, E.; Coletti, F.; Macchietto, S. A Model-Based Method for Visualization, Monitoring, and Diagnosis of Fouling in Heat Exchangers. *Ind. Eng. Chem. Res.* **2020**, *59*, 4602–4619. [[CrossRef](#)]
79. Wang, W.; Watkinson, A.P. Deposition From a Sour Heavy Oil Under Incipient Coking Conditions: Effect of Surface Materials and Temperature. *Heat Transf. Eng.* **2015**, *36*, 623–631. [[CrossRef](#)]
80. Diaz-Bejarano, E.; Coletti, F.; Macchietto, S. Impact of Complex Layering Structures of Organic and Inorganic Foulants on the Thermo-hydraulic Performance of a Single Heat Exchanger Tube: A Simulation Study. *Ind. Eng. Chem. Res.* **2016**, *55*, 10718–10734. [[CrossRef](#)]
81. Diaz-Bejarano, E.; Coletti, F.; Macchietto, S. Detection of changes in fouling behavior by simultaneous monitoring of thermal and hydraulic performance of refinery heat exchangers. *Comput. Aided Process Eng.* **2015**, *37*, 1649–1654.
82. Mozdianfard, M.R.; Behranvand, E. Fouling at post desalter and preflash drum heat exchangers of CDU preheat train. *Appl. Therm. Eng.* **2015**, *89*, 783–794. [[CrossRef](#)]
83. Diaz-Bejarano, E.; Coletti, F.; Macchietto, S. Impact of crude oil fouling composition on the thermo-hydraulic performance of refinery heat exchangers. In Proceedings of the 11th International Conference on Heat Transfer, Fluid Mechanics and Thermodynamics, Skukuza, South Africa, 20–23 July 2015.
84. Diaz-Bejarano, E.; Behranvand, E.; Coletti, F.; Mozdianfard, M.R.; Macchietto, S. Organic and inorganic fouling in heat exchangers—Industrial case study: Analysis of fouling state. *Appl. Energy* **2017**, *206*, 1250–1266. [[CrossRef](#)]
85. Diaz-Bejarano, E.; Behranvand, E.; Coletti, F.; Mozdianfard, M.R.; Macchietto, S. Organic and Inorganic Fouling in Heat Exchangers: Industrial Case Study Analysis of Fouling Rate. *Ind. Eng. Chem. Res.* **2019**, *58*, 228–246. [[CrossRef](#)]
86. Mohammadi, K.; Heidemann, W.; Müller-Steinhagen, H. Numerical Investigation of the Effect of Baffle Orientation on Heat Transfer and Pressure Drop in a Shell and Tube Heat Exchanger With Leakage Flows. *Heat Transf. Eng.* **2009**, *30*, 1123–1135. [[CrossRef](#)]
87. Fahmi, B.; Wolfgang, A.; Matthias, B. Numerical Simulation of the Fouling on Structured Heat Transfer Surfaces (Fouling). In Proceedings of the Heat Exchanger Fouling and Cleaning: Fundamentals and Applications, Santa Fe, NM, USA, 18–22 May 2003.
88. Svendsen, J.A. Mathematical modeling of wax deposition in oil pipeline systems. *AIChE J.* **1993**, *39*, 1377–1388. [[CrossRef](#)]
89. Sileri, D.; Sahu, K.; Ding, H.; Matar, O. Mathematical modelling of asphaltene deposition and removal in crude distillation units. In Proceedings of the International Conference on Heat Exchanger Fouling and Cleaning VIII, Schlading, Austria, 14–19 June 2009; pp. 245–251.
90. Yang, J.; Matar, O.; Hewitt, G.; Zheng, W.; Manchanda, P. Modelling of Fundamental Transfer Processes in Crude-Oil Fouling. In Proceedings of the International Heat Transfer Conference 15, Kyoto, Japan, 10–15 August 2014.
91. Yang, J.; Serratos, M.G.J.; Fari-Arole, D.S.; Muller, E.A.; Matar, O.K. Crude Oil Fouling: Fluid Dynamics, Reactions and Phase Change. *Procedia IUTAM* **2015**, *15*, 186–193. [[CrossRef](#)]
92. Bayat, M.; Aminian, J.; Bazmi, M.; Shahhosseini, S.; Sharifi, K. CFD modeling of fouling in crude oil pre-heaters. *Energy Convers. Manag.* **2012**, *64*, 344–350. [[CrossRef](#)]
93. Yang, M.; Crittenden, B. Use of CFD to Determine Effect of Wire Matrix Inserts on Crude Oil Fouling Conditions. *Heat Transf. Eng.* **2013**, *34*, 769–775. [[CrossRef](#)]
94. Yang, M.; Crittenden, B. Fouling thresholds in bare tubes and tubes fitted with inserts. *Appl. Energy* **2012**, *89*, 67–73. [[CrossRef](#)]
95. Chambon, A.; Anxionnaz-Minvielle, Z.; Fourmigué, J.-F.; Guintrand, N.; Davailles, A.; Ducros, F. Use of Distributed Threshold Fouling Model at Local Scale in Numerical Simulations. *Ind. Eng. Chem. Res.* **2019**, *58*, 15003–15013. [[CrossRef](#)]

96. Haghshenasfard, M.; Hooman, K. CFD modeling of asphaltene deposition rate from crude oil. *J. Pet. Sci. Eng.* **2015**, *128*, 24–32. [[CrossRef](#)]
97. Emani, S.; Ramasamy, M.; Shaari, K.Z.B.K. Effect of Shear Stress on Crude Oil Fouling in a Heat Exchanger Tube Through CFD Simulations. In Proceedings of the 4th International Conference on Process Engineering and Advanced Materials (ICPEAM 2016), Kuala Lumpur, Malaysia, 5–17 August 2016; Volume 148, pp. 1058–1065. [[CrossRef](#)]
98. Emani, S.; Ramasamy, M.; Shaari, K.Z.K. Discrete phase-CFD simulations of asphaltene particles deposition from crude oil in shell and tube heat exchangers. *Appl. Therm. Eng.* **2019**, *149*, 105–118. [[CrossRef](#)]
99. Ghorbani, M.; Maddahian, R. Investigation of asphaltene particles size and distribution on fouling rate in the crude oil preheat train. *J. Pet. Sci. Eng.* **2021**, *196*, 107665. [[CrossRef](#)]
100. Paz, C.; Suarez, E.; Conde, M.; Vence, J. Development of a Computational Fluid Dynamics Model for Predicting Fouling Process Using Dynamic Mesh Model. *Heat Transf. Eng.* **2020**, *41*, 199–207. [[CrossRef](#)]

**Disclaimer/Publisher’s Note:** The statements, opinions and data contained in all publications are solely those of the individual author(s) and contributor(s) and not of MDPI and/or the editor(s). MDPI and/or the editor(s) disclaim responsibility for any injury to people or property resulting from any ideas, methods, instructions or products referred to in the content.